Moment-Rotation Characterization of Cold-Formed Steel Beams Depending on Cross-Section Slenderness

D. Ayhan
Istanbul Technical University, Turkey

B.W. Schafer
Johns Hopkins University, USA

SUMMARY:
The objective of this study is to provide a method to characterize the complete moment-rotation response of cold-formed steel (CFS) beams undergoing local or distortional buckling limit states. Peak strength, and approximations for stiffness loss prior to peak strength, is predicted in current codes for CFS members. However, post-peak M-θ behavior suffers still from a lack of fundamental knowledge. In this research, existing data, obtained by experiments and finite element analysis, are processed to examine the complete M-θ response of cold-formed steel beams. Using a modification of the simplified model introduced in ASCE 41 for pushover analysis, the M-θ response is parameterized into a simple multi-linear curve. The cross-section slenderness, either local or distortional as appropriate, is used as a criterion to predict the parameters of this multi-linear M-θ curve. Accuracy of the proposed M-θ approximation is assessed with finite element models.

Keywords: cold-formed steel beams, local buckling, distortional buckling, moment-rotation response

1. INTRODUCTION

Cold-formed steel (CFS) is becoming a popular building material. However, it is not appropriate to design CFS members or systems according to the specifications concerning hot-rolled steel, since CFS buckling mode shapes, failure mechanisms, strength, stiffness and ductility are all different than the prototypical compact hot-rolled steel member.

Member level strength prediction is well addressed in design codes for CFS; however, less attention has been given to the issue of stiffness. Design specifications (e.g., AISI-S100-07) do provide methods for approximating the reduced stiffness due to local buckling – typically using variations of the effective width method. In addition, AISI-S100-07 Appendix 1 also provides an approach for predicting the stiffness that relies directly on the cross-section slenderness. These stiffness reductions are only valid up to the ultimate strength of the member, and no means are provided for determining the stiffness past the peak strength.

For modelling collapse, particularly under dynamic (seismic) loads, no current method provides guidance on member ductility of CFS members. As a result conservative design philosophies are employed, for example in CFS framed buildings all nonlinearity is assumed to be concentrated in pre-tested shear walls catalogued by the design codes. Without fundamental information on CFS member stiffness and ductility, system modelling for CFS structures to collapse, or under dynamic loads, is impossible. This research attempts to take the initial steps toward providing this needed information, i.e. the moment-rotation response, for CFS members.

The moment-rotation response of CFS beams is known to be highly sensitive to the cross-section slenderness. Here we focus on existing experiments on beams in local and distortional buckling. Existing experiments and finite element analysis in local and distortional buckling are processed as the basis of this study.

1.1. Existing Data

The experimental work realized by Yu and Schafer (2003, 2006, and 2007) is composed of two test series carried out on industry standard CFS C and Z-sections. The testing setup was carefully designed in the first series of tests to allow local buckling failure to form while restricting distortional and lateral-torsional buckling. The corrugated panel attached to the compression flange was removed in the constant moment region so that distortional buckling could occur for the second series. The maximum load as well as the load–displacement curves were determined in these test series to investigate the strength. Twenty-four local and twenty-two distortional buckling tests were selected to analyse member stiffness and ductility.

Shifferaw and Schafer (2010) used centerline dimensions of seventeen cross-sections having $M_{test}>0.95M_y$ from Yu and Schafer (2003, 2006) to develop and validate an ABAQUS nonlinear collapse shell finite element (FE) model. A total of 187 different FE models were completed with different variations in thickness.

1.2. Investigation of current predictions

Using the preceding studies a comparison is made to determine the accuracy of the pre-peak stiffness predictions from the codes. Measured stiffness is compared with predictions based on the Effective Width Method (EWM) and the Direct Strength Method (DSM). Relationships between local and distortional cross-section slenderness, and the observed and predicted secant stiffness are examined.

Table 1: Summary of Test-to-Predicted Ratios for I_{eff} by EWM and DSM

			$k_{secant\text{-}test}/k_{secant\text{-}predicted}$ at									
			δ_{peak}	$0.9\delta_{peak}$	$0.5\delta_{peak}$	$0.2\delta_{peak}$	$0.1\delta_{peak}$	δ_{peak}	$0.9\delta_{peak}$	$0.5\delta_{peak}$	$0.2\delta_{peak}$	$0.1\delta_{peak}$
			TESTS					ABAQUS MODELS				
		n	24	24	21	9	7	76	76	76	76	76
LOCAL	DSM	μ	0.97	1.01	0.99	0.99	1.00	0.62	0.68	0.89	0.96	0.98
		CV	0.15	0.13	0.03	0.01	0.00	0.36	0.35	0.23	0.13	0.07
		min	0.70	0.75	0.93	0.98	1.00	0.06	0.07	0.12	0.28	0.54
		max	1.19	1.23	1.06	1.00	1.00	1.12	1.16	1.02	1.00	1.00
	EWM	μ	1.13	1.17	1.07	0.99	1.00	0.61	0.67	0.89	0.96	0.98
		CV	0.18	0.15	0.07	0.01	0.00	0.34	0.33	0.23	0.13	0.07
		min	0.77	0.83	0.98	0.98	1.00	0.06	0.07	0.12	0.28	0.54
		max	1.54	1.55	1.27	1.00	1.00	0.95	1.01	1.00	1.00	1.00
DISTORTIONAL		n	22	22	20	9	7	78	78	78	78	78
	DSM	μ	0.97	1.00	0.98	0.97	1.00	0.68	0.74	0.93	0.98	0.98
		CV	0.21	0.19	0.11	0.04	0.00	0.34	0.32	0.14	0.05	0.07
		min	0.43	0.46	0.62	0.88	1.00	0.13	0.14	0.25	0.60	0.54
		max	1.43	1.42	1.18	1.01	1.00	1.13	1.18	1.01	1.01	1.00
	EWM	μ	1.03	1.06	1.02	0.98	1.00	0.64	0.70	0.92	0.96	0.98
		CV	0.20	0.19	0.11	0.04	0.00	0.29	0.28	0.14	0.13	0.07
		min	0.46	0.50	0.68	0.89	1.00	0.13	0.14	0.25	0.28	0.54
		max	1.48	1.46	1.20	1.02	1.01	0.92	0.98	1.01	1.00	1.00

Note: n=number of tests used, μ=average, CV=coefficient of variation

A statistical summary comparing EWM and DSM to the measured data is provided in Table 1 for both test and FE models. Focusing on the accuracy of the stiffness prediction at peak displacement (δ_{peak}), Table 1 shows that neither the EWM nor DSM methods provide a highly accurate stiffness prediction. In comparison with the tests of Yu and Schafer (2003, 2006) the DSM approach is modestly more accurate, and arguably simpler than the EWM. Interestingly, although the EWM provides a cross-section specific stiffness prediction its coefficient of variation is still higher than DSM; thus, the scatter is not improved by this additional effort. However, Table 1 shows both methods to be lacking when compared to the FE models; further work is clearly needed.

2. CFS BEAM M-θ BEHAVIOR

The ductile performance of steel structures may be dependent on the ability of its members to dissipate energy by means of hysteretic behaviour. Equating the area under the original curve, which defines the energy dissipated, to the modelled curve is the first aim for the characterization of CFS moment-rotation behaviour. Variations of the Equivalent Energy Elastic Plastic (EEEP) method (Park 1988) were employed to obtain a simplified curve to predict the full nonlinear response of CFS beam. Given that CFS cross-sections are typically locally slender, they have a more complicated and less forgiving moment-rotation (M-θ) response than compact hot-rolled steel beams. Therefore, simple elastic-perfectly plastic response as commonly used in steel analysis is not typically appropriate for CFS members and the shape of the moment-rotation curve has an important effect on characterization of the CFS beam M-θ behaviour The M-θ behaviour of CFS members have a pre-peak fully effective (elastic) range, pre-peak partially effective range, a peak which is typically less than the yield capacity of the beam, and then a post-peak strength-degraded range. Models inpired from ASCE41 M-θ definitions were examined.

2.1. ASCE 41 M-θ definitions

The latest in a series of documents developed to assist engineers with the seismic assessment and rehabilitation of existing buildings (FEMA 273, 1997; FEMA 356, 2000) is ASCE/SEI 41 (2007). These documents provide a comparison of generalized deformation (Δ) and force demands (Q) for different seismic hazards against deformation and force capacities for various performance levels to provide a performance-based seismic engineering framework. ASCE/SEI 41 (2007) provides three basic types of component force-deformation curves (Fig. 1, where Q=M and Δ=θ, all parameters are define in ASCE 41). The acceptance criteria for each type are defined depending on the performance level.

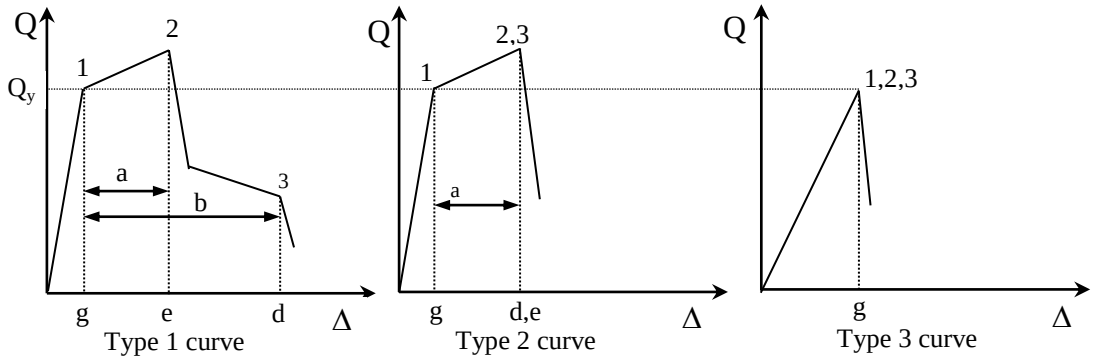

Figure 1: Component force-deformations curves of ASCE 41 (2007)

ASCE 41 does not include explicit predictions for CFS members; therefore, here ASCE 41 backbone 'curve fitting' exercises are realized for CFS members. An ASCE 41 Type 1 curve assumes an elastic range followed by a plastic range including strain hardening, then a post-peak strength degraded range.

2.2. ASCE 41–like models

As Type 1 (Fig. 1) curve includes both pre-peak stiffness loss and post-peak moment degradation features, it was selected as best able to represent the behavior of CFS beams. Accordingly, Model 1, Model 2, and Model 1a (Fig. 2-4) are generated to examine the available data.

2.2.1. Model 1

Model 1 includes pre-peak stiffness loss and a post-peak moment degradation which is described as a combination of post-peak plateau and strength drop (Fig. 2). This shape is defined with 6 points.

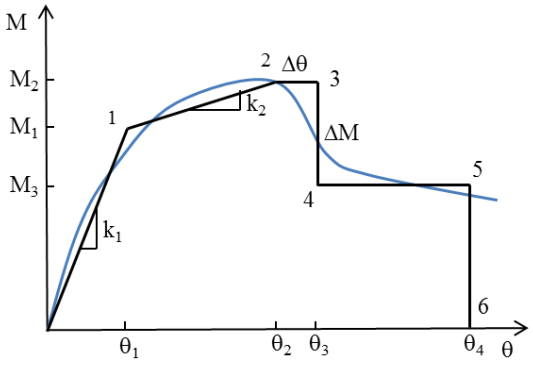

Figure 2: Model 1 backbone curve

2.2.2. Model 2

The shape of Model 2 is differentiated from Model 1 by the post-peak moment degradation. The post-peak region employs a post-peak plateau and stiffness loss (Fig. 3).

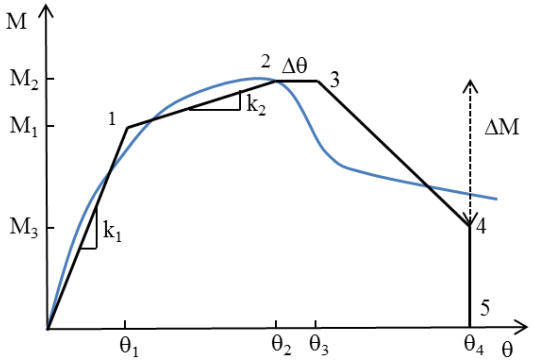

Figure 3: Model 2 backbone curve

2.2.3. Model 1a

The post-peak strength loss is composed of a bilinear stiffness loss curve in Model 1a (Fig. 4). The aim is to reflect real behaviour of CFS beams.

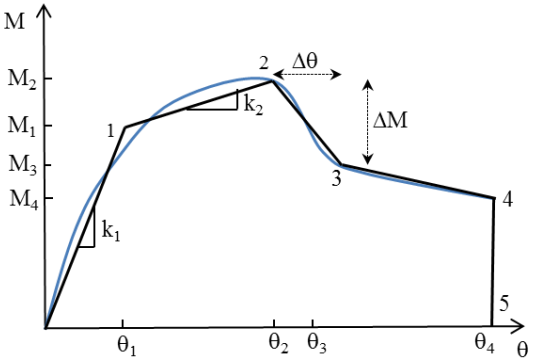

Figure 4: Model 1a backbone curve

2.2.4. Characterization of CFS M-θ curves with ASCE-like models

The test data of Yu and Schafer (2003, 2006) and the FE results of Shifferaw and Schafer (2010) are down-sampled and converted from load-displacement to moment-rotation and then ASCE41-like models are "fit" to the data. The optimization problem, to define the parameters which are needed to characterize CFS moment-rotation response via the Type 1 curve, is solved in MATLAB. The error considered was calculated as the sum of squares of the difference of pre-peak area under the curves and difference of post-peak area under the curves. The key point in selecting from the three moment-rotation models obtained, are the shape of the M-θ curve and its ability to properly capture the energy.

Several "fits" were pursued, four are detailed here. Two of the "fits" use all available data and the others limit the data to only $M_{postpeak}$ >50%M_t. For both, "fits" are realized by either minimizing sum squared error on all 7 model parameters termed the "full fit", or by fitting only k_2, $\Delta\theta$, and ΔM termed the "const. fit". The constrained fit (abbreviated "const. fit") constrains the initial stiffness (k_1) and the peak (θ_2, M_2) as well as the final moment (M_4) to be the same as the test, also only in Model 1a final rotation (θ_4) is also fixed to be the same as the test in the "const. fit".

All models equate pre- and post-peak energy accurately. Model 1a provides a reliable characterization of the M-θ behavior for the four point bending tests and simulations, but no suitable way exists to predict M_4, the post-peak moment capacity of Model 1a. Model 1 provides accurate results as error residuals are reasonable (generally less than $1x10^{-10}$) and the M-θ backbone follows a similar path to the available data. Adaptation of Model 1 is recommended.

2.3. Design expressions for CFS M-q predictions

A systematic design method for predicting the parameters of the M-θ backbone curve, applicable to all CFS beams failing in either local or distortional buckling is needed. The Model 1 (Fig. 2) "const. fit" with the data limited to $M_{postpeak}$ >50%M_t is employed for the parameterization conducted here. The objective is to create functional relationships that predict the Model 1 parameters, as predicted in the preceding optimization. M-θ fits are provided in CFS-NEES RR02 (Ayhan and Schafer, 2012).

Table 2: Design expressions for local and distortional buckling

	local	distortional
	$\lambda_\ell = \sqrt{\frac{M_y}{M_{cr\ell}}}$	$\lambda_d = \sqrt{\frac{M_y}{M_{crd}}}$
rotation	$\frac{\theta_1}{\theta_y} = \frac{M_1}{k_1\theta_y} = \frac{M_1}{k_e\theta_y} = \frac{M_1}{M_y}$ (note, M_1 given below)	$\frac{\theta_1}{\theta_y} = \frac{M_1}{k_1\theta_y} = \frac{M_1}{k_e\theta_y} = \frac{M_1}{M_y}$
rotation	$\frac{\theta_2}{\theta_y} = \frac{1}{\lambda_\ell} \le \frac{M_2}{k_e}$	$\frac{\theta_2}{\theta_y} = \left(\frac{1}{\lambda_d}\right)^{1.4}$
rotation	$\theta_3 = \theta_2 + \Delta\theta$, where $\Delta\theta$ is: $\frac{\Delta\theta}{\theta_y} = \begin{cases} \left(\frac{0.776}{\lambda_\ell}\right) - 1 & \text{if } \lambda_\ell < 0.776 \\ 0 & \text{if } \lambda_\ell \ge 0.776 \end{cases}$	$\theta_3 = \theta_2 + \Delta\theta$, where $\Delta\theta$ is: $\frac{\Delta\theta}{\theta_y} = \begin{cases} \left(\frac{0.673}{\lambda_d}\right) - 1 & \text{if } \lambda_d < 0.673 \\ 0 & \text{if } \lambda_d \ge 0.673 \end{cases}$
rotation	$\frac{\theta_4}{\theta_y} = \begin{cases} 1.5\frac{1}{\lambda_\ell} & \text{if } \lambda_\ell > 1 \\ 1.5\left(\frac{1}{\lambda_\ell}\right)^{1/4\lambda_l} & \text{if } \lambda_\ell \le 1 \end{cases}$	$\frac{\theta_4}{\theta_y} = \begin{cases} 1.5\left(\frac{1}{\lambda_d}\right)^{1.4} & \text{if } \lambda_d > 1 \\ 1.5\left(\frac{1}{\lambda_d}\right)^{1.4/\lambda_d} & \text{if } \lambda_d \le 1 \end{cases}$
moment	$\frac{M_1}{M_y} = \left\{ \begin{cases} 1 & \text{if } \lambda_\ell < 0.650 \\ \left(\frac{0.650}{\lambda_\ell}\right)^2 & \text{if } \lambda_\ell \ge 0.650 \end{cases} \right\} \le \frac{M_2}{M_y}$	$\frac{M_1}{M_y} = \left\{ \begin{cases} 1 & \text{if } \lambda_\ell < 0.600 \\ \left(\frac{0.600}{\lambda_d}\right)^2 & \text{if } \lambda_\ell \ge 0.600 \end{cases} \right\} \le \frac{M_2}{M_y}$
moment	$\frac{M_2}{M_y} = \frac{M_{n\ell}}{M_y}$ where $M_{n\ell}$ is per AISI - S100, i.e.:	$\frac{M_2}{M_y} = \frac{M_{nd}}{M_y}$ where M_{nd} is per AISI - S100, i.e.:
moment	$\frac{M_2}{M_y} = \begin{cases} 1 + \left(1 - \frac{1}{C_{yl}^2}\right)\frac{(M_p - M_y)}{M_y} \quad and \quad C_{yl} = \sqrt{\frac{0.776}{\lambda_l}} \le 3 \quad if \quad \lambda_l < 0.776 \\ \left(1 - 0.15\left(\frac{1}{\lambda_l^2}\right)^{0.4}\right)\left(\frac{1}{\lambda_l^2}\right)^{0.4} \quad if \quad \lambda_l > 0.776 \end{cases}$	$\frac{M_2}{M_y} = \begin{cases} 1 + \left(1 - \frac{1}{C_{yd}^2}\right)\frac{(M_p - M_y)}{M_y} \text{ and } C_{yd} = \sqrt{\frac{0.673}{\lambda_d}} \le 3 & \text{if } \lambda_d < 0.673 \\ \left(1 - 0.22\left(\frac{1}{\lambda_\ell^2}\right)^{0.5}\right)\left(\frac{1}{\lambda_\ell^2}\right)^{0.5} & \text{if } \lambda_d \ge 0.673 \end{cases}$
moment	$M_3 = M_2 - \Delta M$, where ΔM is: $\frac{\Delta M}{M_2} = 1 - 1/\left(\frac{\lambda_\ell}{0.776} + 1\right)^{1.1} \le 0.5$	$M_3 = M_2 - \Delta M$, where ΔM is: $\frac{\Delta M}{M_2} = 1 - 1/\left(\frac{\lambda_d}{0.673} + 1\right)^{1.4} \le 0.5$

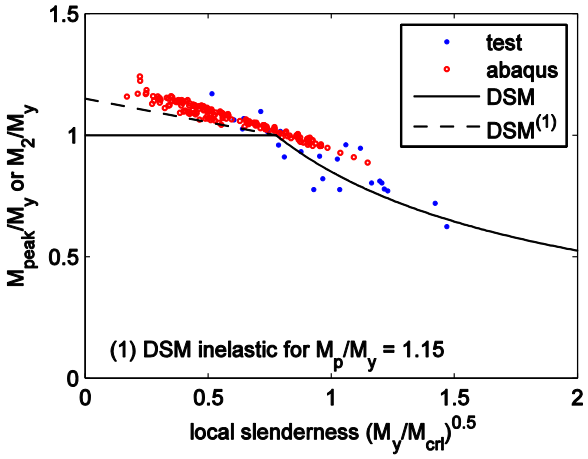

(a) peak moment (M_{peak} or M_2)

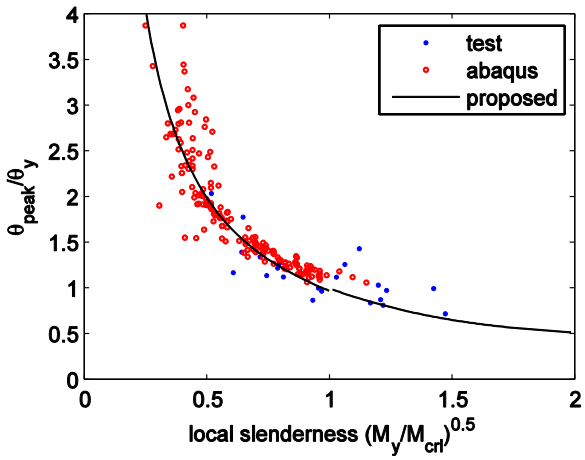

(b) rotation at M_2 (θ_{peak} or θ_2)

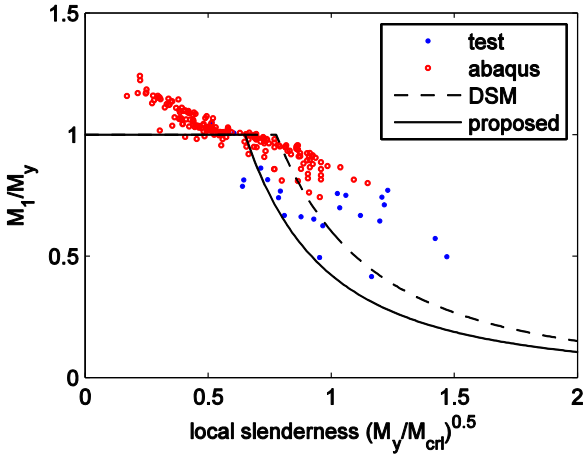

(c) fully effective moment (M_1)

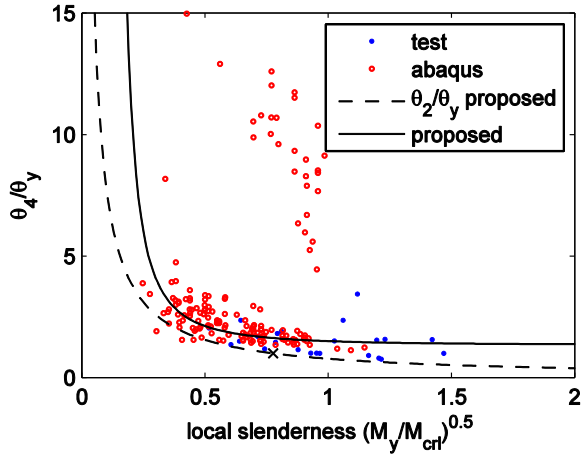

(d) maximum rotation (θ_4)

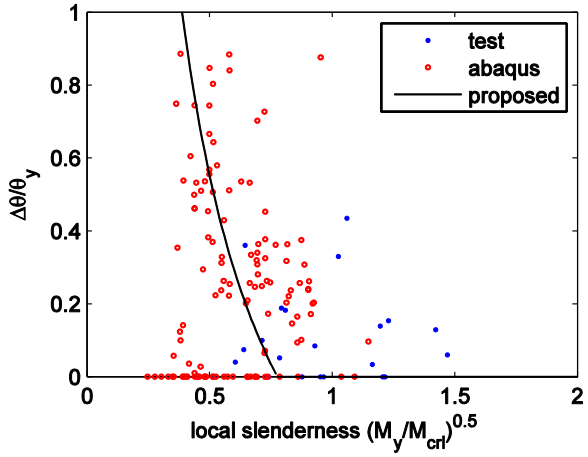

(e) inelastic plateau ($\Delta\theta$)

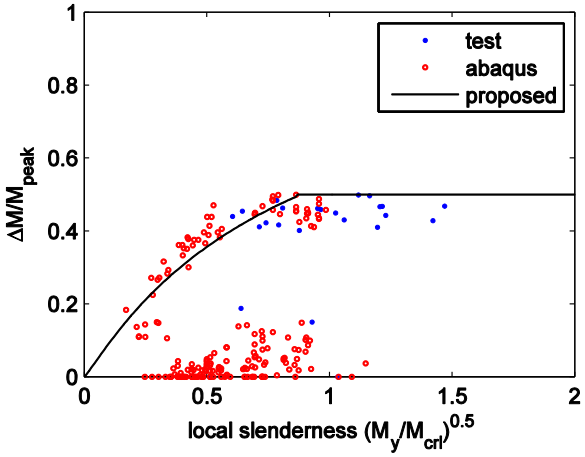

(f) post-peak moment drop (ΔM)

Figure 5: CFS-NEES Model 1a parmaters for available data as a function of local slenderness, proposed design expressions indicated by solid lines

Due to the large range of observed M-θ behavior it is not possible to provide fixed values for the Model 1 parameters as is typical, for example, in ASCE 41. However, existing design does provide insights on how to predict many of the Model 1 parameters. For example, the peak moment capacity (M_2), is known to be well predicted by the Direct Strength Method (DSM) of AISI-S100. DSM uses cross-section slenderness (λ) as the key variable for predicting strength, as shown in Table 2. Where

$$\lambda = \sqrt{\frac{M_y}{M_{cr}}} \tag{2.1}$$

and M_y is the elastic yield moment, and M_{cr} is the elastic critical buckling moment, either local or distortional. All the key parameters are expressed depending on cross-section slenderness (λ).

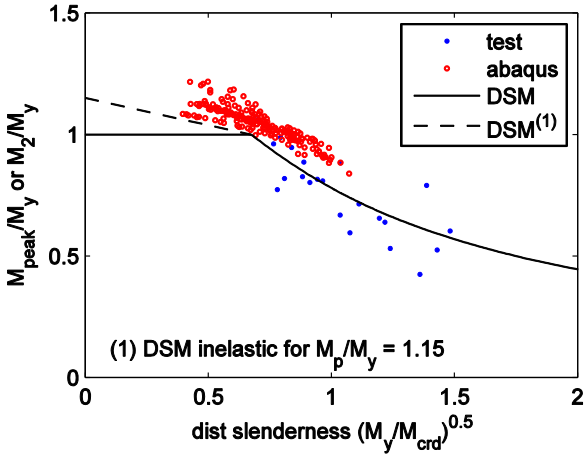

(a) peak moment (M_{peak} or M_2)

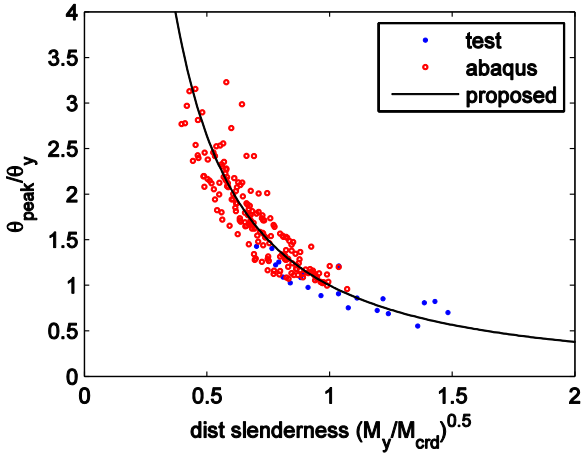

(b) rotation at M_2 (θ_{peak} or θ_2)

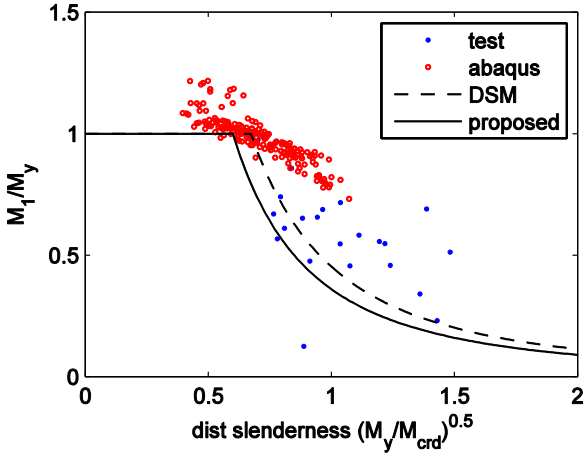

(c) fully effective moment (M_1)

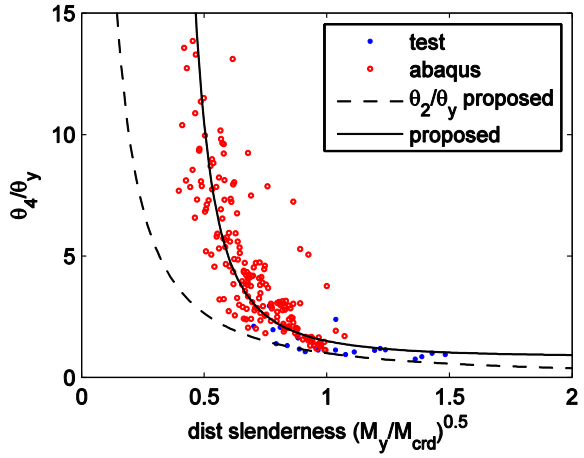

(d) maximum rotation (θ_4)

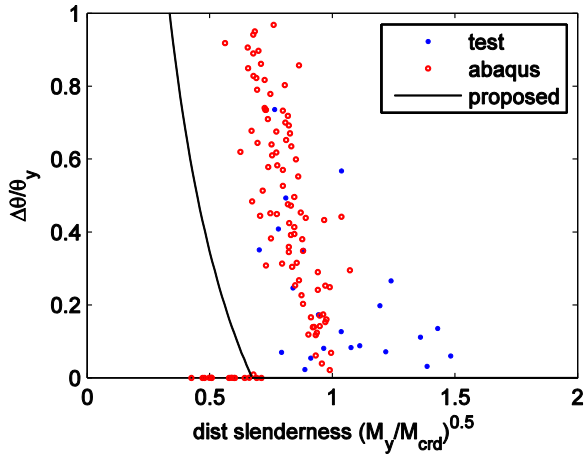

(e) inelastic plateau ($\Delta\theta$)

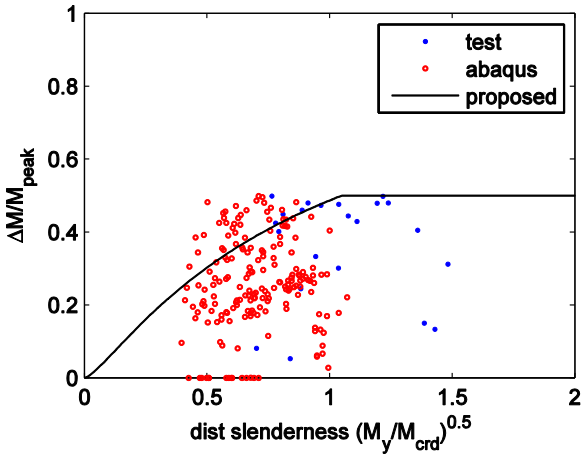

(f) post-peak moment drop (ΔM)

Figure 6: CFS-NEES Model 1 parmaters for available data as a function of distortional slenderness, proposed design expressions indicated by solid lines

Table 2 provides a summary of the proposed design expressions. These simple expressions provide a means to determine the reduced stiffness that occurs due to local or distortional buckling, unlike existing stiffness predictions, this stiffness method is decoupled from the strength prediction. For example, the expression for prediction of M_1 implies that the local slenderness must be as small as 0.65 and distortional slenderness 0.60 for the section to be fully effective. Performance of these expressions against the available data is provided in Fig. 5 and Fig 6, respectively for local and distortional buckling and statistically summarized in Table 3.

3. ACCURACY OF DESIGN EXPRESSIONS

A quantitative assessment of the accuracy of the prediction method is provided in Table 3. Consistent with the figures, variation (standard deviation) can sometimes be significant; however, taken in total the method performs surprisingly well. Exploration of Fig. 5f and 6f shows that statistics for moment drop which are greater than 20% of M_2 produce better results as shown in the last column of Table 2.

Table 3: Test-to-predicted statistics for proposed design method

			ratio of test (or FE) - to - predicted for							
			Energy		fully eff. limit	eff. k	peak		drop	
			Pre-peak	Post-peak	M_1	k_{sec}	θ_2	M_2	ΔM	for $\Delta M>0.20M2$
local	tests	mean	1.00	1.03	1.36	1.00	1.06	1.03	0.84	0.97
		st. dev.	0.32	0.61	0.13	0.15	0.20	0.08	0.32	0.09
	FE models	mean	1.18	1.09	1.21	1.01	1.06	1.046	0.400	1.07
		st. dev.	0.71	1.06	0.14	0.15	0.20	0.024	0.467	0.10
	all data	mean	1.16	1.08	1.23	1.01	1.06	1.04	0.45	1.06
		st. dev.	0.66	1.01	0.14	0.15	0.20	0.03	0.45	0.10
distortional	tests	mean	0.89	0.84	1.26	1.01	0.98	0.98	0.75	0.86
		st. dev.	0.26	0.41	0.00	0.16	0.16	0.13	0.31	0.21
	FE models	mean	1.10	1.56	1.21	1.08	1.07	1.10	0.73	0.91
		st. dev.	0.55	0.81	0.07	0.19	0.40	0.04	0.37	0.27
	all data	mean	1.08	1.48	1.21	1.08	1.06	1.08	0.73	0.90
		st. dev.	0.52	0.77	0.07	0.19	0.39	0.06	0.37	0.26

Table 4: Comparison of design expressions results with EWM and DSM for pre-peak stiffness

		$k_{secant\text{-}measured}/k_{secant\text{-}predicted}$ at									
		δ_{peak}	$0.9\delta_{peak}$	$0.8\delta_{peak}$	$0.7\delta_{peak}$	$0.6\delta_{peak}$	$0.5\delta_{peak}$	$0.4\delta_{peak}$	$0.3\delta_{peak}$	$0.2\delta_{peak}$	$0.1\delta_{peak}$
mean	***LOCAL BUCKLING FE models***										
	DSM	0.62	0.68	0.74	0.79	0.84	0.88	0.92	0.95	0.97	1.00
	EWM	0.61	0.67	0.73	0.79	0.84	0.89	0.92	0.95	0.97	1.00
	D.Exp	0.98	1.03	1.06	1.06	1.03	1.01	1.00	1.01	1.02	1.02
	LOCAL BUCKLING tests										
	DSM	0.97	1.01	1.02	1.02	1.01	0.99	0.98	0.98	0.99	1.00
	EWM	1.13	1.17	1.16	1.15	1.11	1.07	1.03	1.00	0.99	1.00
	D.Exp	1.00	1.03	1.04	1.02	1.00	0.98	0.98	0.96	0.96	1.00
	DIST BUCKLING FE models										
	DSM	0.71	0.77	0.83	0.88	0.91	0.94	0.96	0.98	0.99	1.00
	EWM	0.65	0.71	0.77	0.83	0.89	0.93	0.96	0.97	0.99	1.00
	D.Exp.	1.07	1.12	1.15	1.15	1.12	1.06	1.01	1.00	1.00	1.00
	DIST BUCKLING tests										
	DSM	0.97	1.00	1.01	1.01	0.99	0.98	0.97	0.96	0.97	1.00
	EWM	1.03	1.06	1.07	1.07	1.04	1.02	0.99	0.99	0.98	1.00
	D.Exp.	1.02	1.05	1.06	1.06	1.03	1.00	0.97	0.97	0.97	1.00

Table 4 provides a comparison of pre-peak stiffness between the traditional methods (EWM and DSM) and the newly proposed characterization, abbreviated as "D.Exp" in the table. The new expressions are simple in form and provide much improved accuracy over the available approaches. These new expressions are recommended for design.

4. EXAMPLE FOR APPLICATION OF DESIGN EXPRESSION

An idealization of the beam behaviour of Fig. 7a is realized with the nonlinear spring model (rigid bar) of Fig. 7b. The nonlinear spring characteristics of Fig. 7b are defined according to the predicted moment-rotation behaviour for CFS beams as predicted by the expressions developed herein. ABAQUS has been adopted as the computational tool.

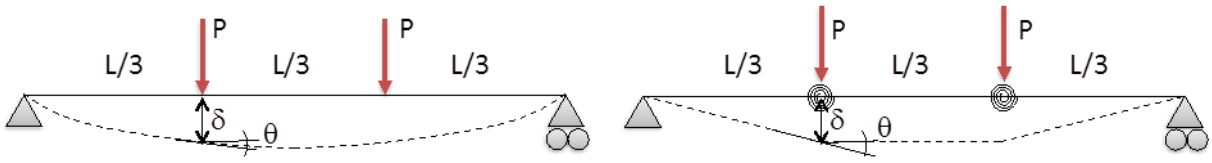

(a) variable definitions and continuous model (b) two parameter lumped rotational spring model

Figure 7: Conversion of measured data in 4 point bending test

Several cross-sections from the local and distortional buckling tests are investigated. The results for two such analyses are compared in Fig. 8. The moment-rotation curve of the ABAQUS bar-spring model perfectly matches the curve assigned to it from the design expressions. These figures also demonstrate how the design expressions compare to the actual and Model 1 fitted data.

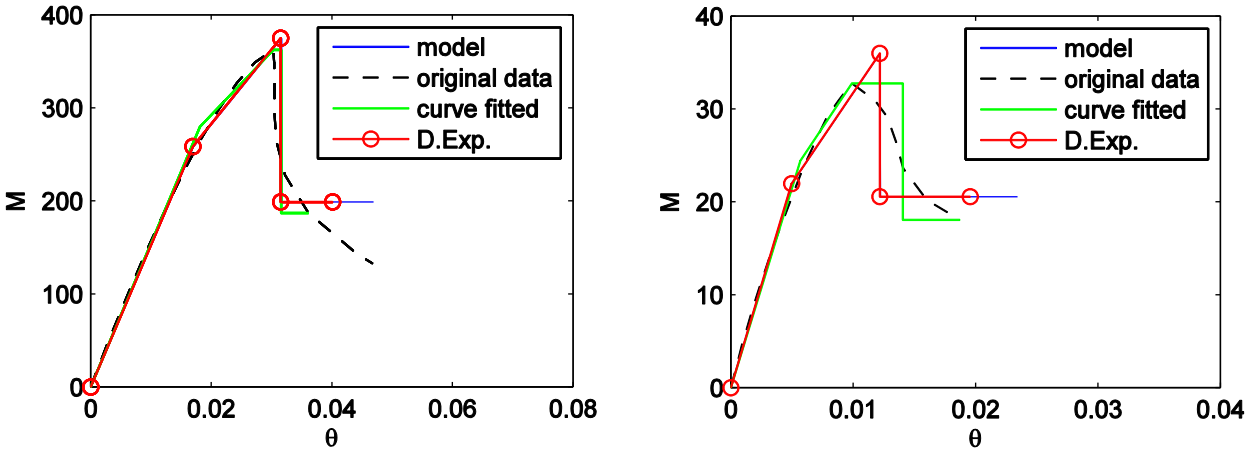

(a) 8.5Z092-4E2W (L3) (b) D8Z033-1E2W (D16)

Figure 8: Verification of M-θ curve for test specimens

5. CONCLUSION AND FUTURE WORK

Stiffness and ductility of cold-formed steel members are fundamental quantities for predicting the collapse behaviour of structures comprised of cold-formed steel. However, given the complexity in predicting peak strength, little attention has been paid to design procedures for predicting stiffness and ductility. Here we utilize existing tests and finite element models to characterize the backbone M-θ response of cold-formed steel beams failing in local and distortional buckling limit states. Simplified multi-linear models in the spirit of ASCE 41 formulations are fit to existing data by insuring pre-peak and post-peak energy balance is maintained between the model and the original data. The derived model parameters, e.g. the moment at which pre-peak nonlinear stiffness engages (M_1) or the available

rotation at a post-peak moment level 50% of the peak value (θ_4) are then examined to determine if a simple method may be used in their prediction. It is found that local and distortional cross-sectional slenderness are adequate explanatory variables for parameterizing the simplified M-θ model parameters – and simple design expressions are developed for predicting unique M-θ curves for all cold-formed steel cross-sections in local or distortional buckling. The developed expressions are shown to adequately predict the available data and provide an improvement for pre-peak stiffness prediction when compared to existing methods. In addition, for the first time, post-peak predictions of ductility are available for cold-formed steel beams. Significant future work remains, most notably (a) developing companion expressions that address moment-curvature instead of moment-rotation to provide a more fundamental set of expressions for implementation in analysis, (b) implementing the proposed expressions in an analysis framework such that ASCE 41 style pushover analysis can be explored in real structures, and (c) performing additional cyclic testing to verify and expand the proposed design method based on monotonic testing to complete cyclic response.

AKCNOWLEDGEMENTS

This report was prepared as part of the U.S. National Science Foundation sponsored CFS-NEES project: NSF-CMMI-1041578: NEESR-CR: Enabling Performance-Based Seismic Design of Multi-Story Cold-Formed Steel Structures. The project also received supplementary support and funding from the American Iron and Steel Institute. Project updates are available at www.ce.jhu.edu/cfsnees. Any opinions, findings, and conclusions or recommendations expressed in this publication are those of the author(s) and do not necessarily reflect the views of the National Science Foundation, nor the American Iron and Steel Institute.

REFERENCES

ABAQUS. (2010). ABAQUS/Standard User's Manual, Version 6.9, ABAQUS, Inc., Pawtucket, RI.

American Iron and Steel Institute (AISI). (2007). North American Specification for the Design of Cold-Formed Steel Structural Members; and 2007 edition: Commentary on the Specification, Washington, D.C.

American Iron and Steel Institute (AISI). (2007). Supplement 2007 to the North American Specification for the Design of Cold-Formed Steel Structural Members, 2007 edition, Appendix 1, Design of Cold-Formed Steel Structural Members Using Direct Strength Method, Washington, D.C.

American Society of Civil Engineers (ASCE/SEI 41-06). (2007). Seismic Rehabilitation of Existing Buildings, Reston, Virginia.

Ayhan, D, Schafer, BW (2011). "Impact of cross-section stability on member stability and ductility". Structural Stability Research Council (AISI).

Ayhan, D, Schafer, B.W. (2011). "Ductility and stiffness of cold formed steel members: Guidance for prediction based on cross-section stability". Eurosteel, Budapest, Hungary.

Ayhan, D, Schafer, BW (2012). "Characterization of moment-rotation response of cold-formed steel beams", Structural Stability Research Council (AISI).

Ayhan, D, Schafer, BW (2012). "Moment-Rotation Characterization of Cold-Formed Steel Beams". NSF-CMMI-1041578: NEESR-CR: Enabling Performance-Based Seismic Design of Multi-Story Cold-Formed Steel Structures, CFS-NEES - RR.

MATLAB (2009). Version 7.9.0.529, The MathWorks Inc

Park, R. (1988). "Ductility Evaluation from Laboratory and Analytical Testing". 9th World Conference on Earthquake Engineering, Tokyo-Kyoto, Japan, Vol.VIII.

Shifferaw, Y., Schafer, B.W. (2011). "Inelastic Bending Capacity of Cold-Formed Steel Members". ASCE, Journal of Structural Engineering.

Schafer, B.W. (2008). "Review: The Direct Strength Method of cold-formed steel member design". *J. Constr. Steel Res.*, 64(7-8), 766-778.

Yu, C., Schafer, B.W. (2003). "Local buckling Test on Cold-Formed Steel Beams." Journal of Structural Engineering. ASCE, 129 (12) 1596-1606.

Yu, C, Schafer, B.W., (2006). "Distortional buckling tests on cold formed steel beams". Journal of Structural Engineering, ASCE, 515-528.